PerTPV – Perovskite thin film photovoltaics

Grant agreement 763977

D2.7

Single junction solar cells based on perovskite absorbers with 1.2 eV and 1.85 eV, having efficiencies above 23% and 18% respectively

WP2

Lead beneficiary: UOXF
Authors: Prof Henry Snaith
Delivery date: 31/3/2021
Nature: Demonstrator
Confidentiality level: Public

The PerTPV project has received funding from the European Union's Horizon 2020 research and innovation programme under grant agreement No 763977.

Revision History

Author Name, Partner short name	Description	Date
Henry Snaith (UOXF)	Draft deliverable	30/3/2021
Henry Snaith (UOXF)	Revision 1	31/03/2021
Henk Bolink	Revision 2	01/04/2021
Henry Snaith (UOXF)	Final version	01/04/2021

Contents

The PerTPV project has received funding from the European Union's Horizon 2020 research and innovation programme under grant agreement No 763977.

1. Description and objectives

PerTPV is focused on developing and delivering the ideal and stable perovskite absorbers for both tandem and single junction perovskite cells. The aim of D2.2 is to report on two types of single junction solar cells: one with a narrow bandgap of ~1.2 eV that will eventually form the bottom sub-cell in an all perovskite tandem, and one based on a wide bang gap absorber of ~1.8 eV, which would be used at the top-cell in tandem devices.

In addition, despite small area cells have demonstrated high efficiencies and stabilities, they are mainly prepared using methods that are incompatible for large volume production. A second challenge is therefore to enable suitable stability and performance using processes that are up-scalable to production. Within PerTPV we have explored processes to deposit multicomponent perovskite absorber with different bandgaps (Eg) from both solution and vapour phase, with the aim to achieve similar properties to today's best-in-class perovskite solar cells.

For the wide band gap material we are targeting materials with band gaps of 1.8 +/- 0.05 eV as the ideal range for the top cell. The second material, having a band gap of ~1.8 eV, has achieved PCE of 17% when deposited via solution (1.79 eV gap), and 16.5 % from vacuum deposition (1.75 eV gap). In the project, we have also developed new hole-transport material self-assembled monolayers, which have delivered a significant increase in the open-circuit voltage attainable with these wide band gap devices. Details are discussed in section 2.

The narrow band gap material, having a band gap of ~1.23 eV, is a binary lead-tin perovskite. In the first period of the project we assessed both solution processed and vapour deposited Pb:Sn perovskites, but found that the reproducibility and overall efficiency of the vapour phase deposited material was much lower than the solution processed perovskite. Therefore in this second period, a focus has been on the solution processed absorber. Initially, only Oxford University had expertise in processing the Pb:Sn perovskite, however, through a series of physics researcher exchanges and information exchange, now UVEG, CSEM and IIT-Millan can all fabricate competitively efficient Pb:Sn perovskite cells. This has helped the project considerably in the next steps of developing the tandem cells, since a lot of development work is feasible within each institution, without having to rely on low gap cells being shipped from Oxford University. In terms of cell performance, a maximum single junction solar cell power conversion efficiency (PCE) of 18% has been achieved. The material and device characteristics are discussed in detail in section 3.

2. Wide gap perovskite cells

2.1 Evaporated Wide Gap (1.8eV) Perovskite Cells

The perovskite films with increasing bandgap were tested in p-i-n perovskite solar cells with the structure ITO/MoO_3 (5 nm)/TaTm (10 nm)/perovskite (500 nm)/C60/BCP (8 nm)/Ag, where TaTm is the hole transport material (HTM) *N*,*N*,*N*',*N*'-Tetra([1,1'-biphenyl]-4-yl)[1,1':4',1''-terphenyl]-4,4''-diamine, C60 is the electron transport material and BCP is the electrode interlayer bathocuproine. The external quantum efficiency (EQE, Figure 2.1a) spectra were found to be similarly high (in the 0.8 - 0.9 range) for the four materials through the whole visible spectrum. The onset of the spectral response in

The PerTPV project has received funding from the European Union's Horizon 2020 research and innovation programme under grant agreement No 763977.

the low energy regime follows the trend expected from the perovskites optical absorption and bandgap (D1.7), i.e. the EQE onset shifts to lower wavelengths when the content of bromide is increased. The corresponding short circuit currents (J_{sc}), calculated by integration of the EQE over the global AM1.5G solar spectra, decrease from 18.3 to 16.5 mA cm^{-2} when widening the bandgap from 1.70 eV to 1.77 eV. These values agree with those extracted from current-density vs. voltage (J-V) curves under simulated solar illumination, depicted in Figure 2.1b.

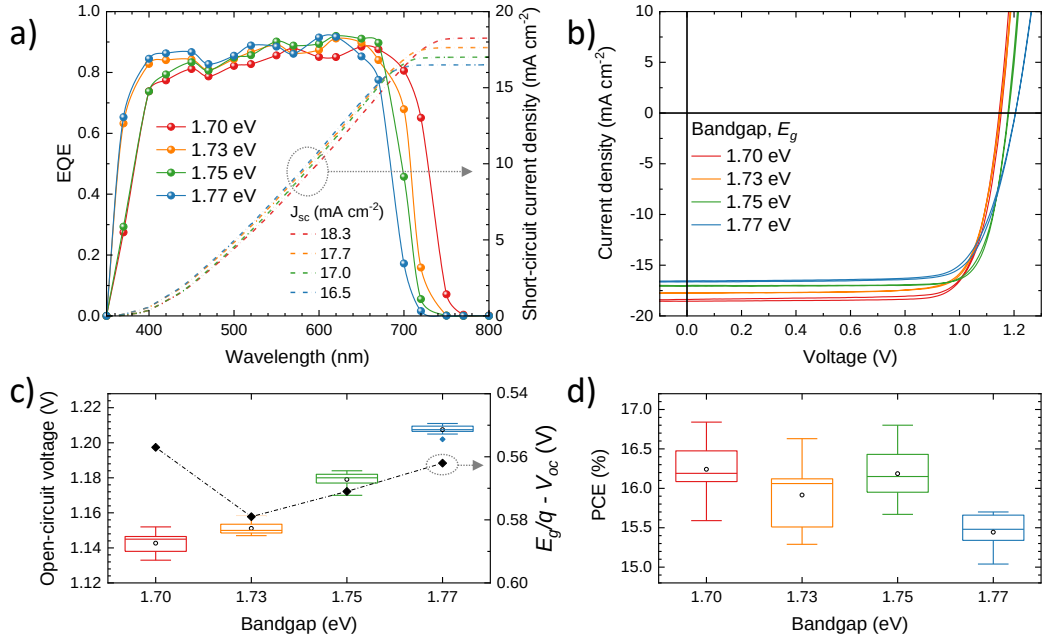

Figure 2.1. Characterization of wide-bandgap perovskite solar cells with $FA_{1-n}Cs_nPb(I_{1-x}Br_x)_3$ absorbers in p-i-n configuration. (a) External quantum efficiency (EQE) spectra (line and symbols) and corresponding short-circuit current density (J_{sc}, dotted lines) calculated by integration of each EQE spectrum with the global AM1.5G solar spectrum. (b) J-V curves under simulated solar illumination recorded in forward (from short to open circuit) and reverse (from open to short circuit) bias for representative pixels. Summary of the (c) open-circuit voltage (V_{oc}) and (d) power conversion efficiency (PCE) measured for perovskite solar cells as a function of the bandgap determined from Tauc analysis. In the right axis in (c), the open-circuit voltage deficit ($E_g/q - V_{oc}$) is also reported (lines are guides to the eye).

The characteristic PV parameters are reported in Table 1. All solar cells showed a high fill factor (FF, between 76 and 80 % on average), indicating an efficient charge extraction of the photogenerated charge carriers. We also observed negligible hysteresis in between the forward and reverse scans, which suggests that either ion migration or interface recombination (or both) are suppressed in these perovskite solar cells. More interesting is the trend of the measured V_{oc}, which scales with the perovskite bandgap (Figure 2.1), going on average from 1.14 V to 1.21 V for the 1.70 eV and 1.77 eV absorber, respectively going from 1.14 V for the 1.70 eV absorber to 1.21 V for the largest 1.77 eV bandgap, on average. The corresponding V_{oc} deficit, defined as (E_g/q-V_{oc}), was found to be rather large (0.56-0.58 V) and constant through the series of devices, indicating a common origin of the non-radiative recombination channels. Although far from the radiative limit for these semiconductors (see discussion below), these values are the highest voltages obtained for wide-bandgap mixed cation/halide perovskite solar cells deposited by vacuum deposition.

The PerTPV project has received funding from the European Union's Horizon 2020 research and innovation programme under grant agreement No 763977.

Table 2.1. Average photovoltaic parameters with standard deviation extracted from J-V curves under simulated solar illumination from wide-bandgap perovskite solar cells with $FA_{1-n}Cs_nPb(I_{1-x}Br_x)_3$ in p-i-n configuration. At least 12 cells for each bandgap have been tested.

Composition	*E_g (eV)*	*J_{sc} (mA cm^{-2})*	*FF (%)*	*V_{oc} (mV)*	*PCE (%)*
$FA_{0.74}Cs_{0.26}Pb(I_{0.86}Br_{0.14})_3$	1.70	18.3 ± 0.2	77.5 ± 0.9	1142 ± 6	16.2 ± 0.3
$FA_{0.71}Cs_{0.29}Pb(I_{0.76}Br_{0.24})_3$	1.73	17.7 ± 0.1	77.5 ± 1.2	1151 ± 3	15.9 ± 0.4
$FA_{0.65}Cs_{0.35}Pb(I_{0.73}Br_{0.27})_3$	1.75	17.0 ± 0.1	80.3 ± 0.8	1179 ± 4	16.2 ± 0.3
$FA_{0.61}Cs_{0.39}Pb(I_{0.70}Br_{0.30})_3$	1.77	16.6 ± 0.1	76.1 ± 0.8	1208 ± 2	15.5 ± 0.2

Overall, our wide-bandgap vacuum-deposited perovskite solar cells show PCEs of about 16% for bandgaps in the 1.70-1.75 eV range. The best pixels were obtained for the wide-bandgap perovskite with E_g = 1.75 eV, with maximum PCE exceeding 16.5%. The reduction in efficiency observed for the solar cells with the highest bromide content are partially expected due to the increased bandgap (1.77 eV), although a small decrease in FF also contributes to the efficiency reduction. These performance details are tabulated in Table 2.1.

We finally evaluated the stability of the most efficient solar cells based on $FA_{1-n}Cs_nPb(I_{1-x}Br_x)_3$ perovskites with E_g = 1.75 eV. Both the shelf life (in the dark) and the operational stability under illumination were evaluated. The devices were encapsulated with a UV-curable resin and a glass slide, and the stability was evaluated in a nitrogen atmosphere to minimize the effect of environmental factors on the degradation. For the shelf-life stability, the *J-V* characteristics under 1-sun illumination were recorded periodically at room temperature (Figure 2.2a). After 500 hours of storage (3 weeks), the PCE was found unvaried from the initial value, indicating an overall good stability of the perovskite film within the device structure used here. To evaluate the operational stability, the devices were maintained at their maximum power point (MPP) under simulated 1-sun equivalent illumination with white LEDs at RT (25 ºC) in nitrogen (Figure 2.2b). Under these operational conditions the solar cell exhibited a remarkable stability, maintaining 90% of the initial PCE after 340 hours (more than 2 weeks) of continuous operation.

The PerTPV project has received funding from the European Union's Horizon 2020 research and innovation programme under grant agreement No 763977.

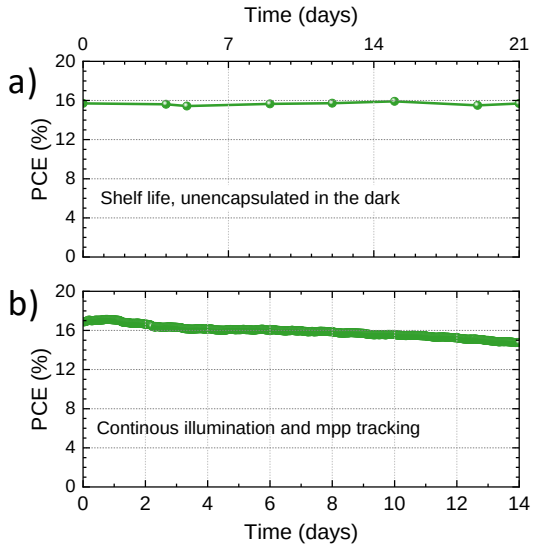

Figure 2.2. Stability assessment of wide-bandgap $FA_{0.65}Cs_{0.35}Pb(I_{0.73}Br_{0.27})_3$ perovskites solar cells with E_g = 1.75 eV, performed on encapsulated devices in nitrogen atmosphere. (a) Shelf-life measurements for devices kept in the dark. (b) Constant maximum power point tracking under continuous illumination.

2.2 Solution processed wide gap perovskite cells:

For the solution processed solar cells, we found that a composition of $FA_{0.83}Cs_{0.17}Pb(I_{0.6}Br_{0.4})$, processed via the anti-solvent quenching route resulted in the ideal band gap of 1.8eV for all perovskite tandem cell applications. With the addition of an ionic additive, which we found supressed non-radiative recombination and both the hole-transport material (HTM) and electron transport layer (ETL) contacts (See D1.7), we have delivered an increase open-circuit voltage and an increase in the average cell efficiency from ~13.6% to 15.6%. Upon further modification of the perovskite-ETL interface with the deposition of a thin Li-F layer, the solar cell fill factor was increased and the average power conversion efficiency increased to ~16.7%. The record cells are over 17% efficiency. We show these results in Figure 2.3.

The PerTPV project has received funding from the European Union's Horizon 2020 research and innovation programme under grant agreement No 763977.

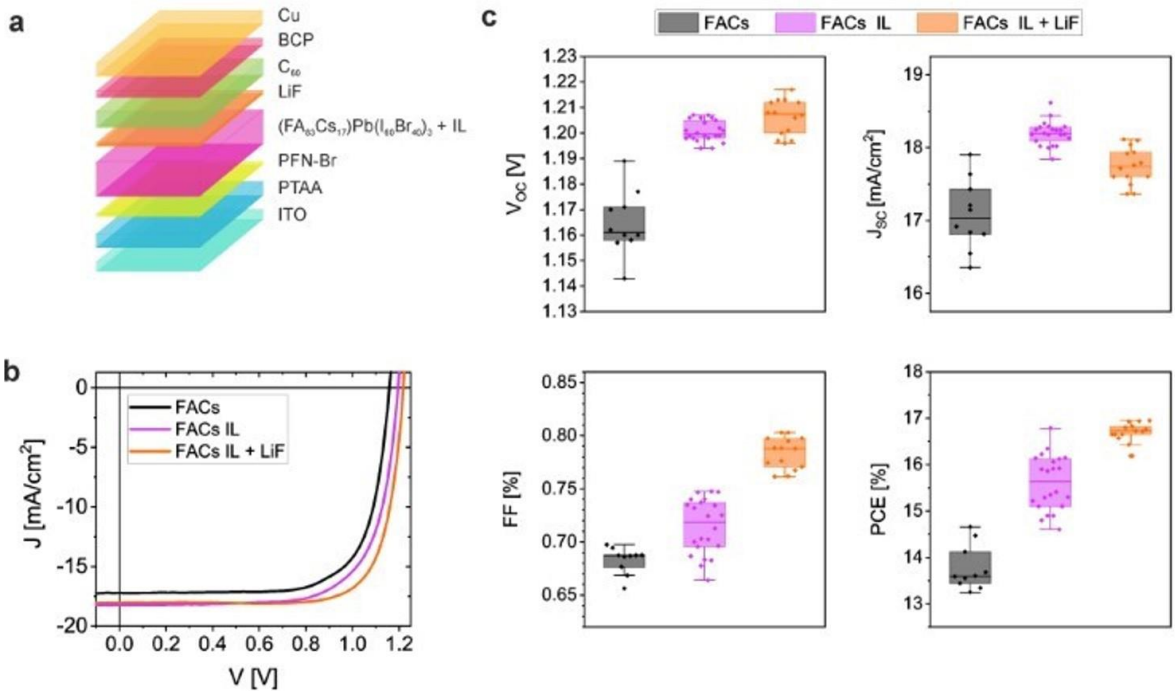

Figure 2.3: Photovoltaic device performance. a) Typical device architecture utilized in this study. b) Exemplary JV curves for the three type of devices investigated. c) Statistics of reference FACs based perovskite solar cells, ionic additive (IL) containing devices and IL containing devices implementing a LiF interlayer.

2.3 Self-assembled Monolayer (SAM) hole-transporter for high efficiency wide gap perovskite cells:

For the analysis of SAM materials on solar cell level, focus was placed on the simple single junction device stack glass/ITO/HTM/perovskite/C_{60}/SnO_2/Ag, with the SnO_2 later serving as a buffer layer for indium zinc oxide (IZO) sputtering in case fabrication of tandem solar cells is undertaken in the future. The SAM molecules can be deposited on transparent conductive oxides via spin-coating or by dipping the substrate into the solution, both yielding layers of comparable properties, combining high reproducibility and ease of fabrication. From the testing results it can be observed that different spacer lengths mainly affect the fill factor (Figure 2.4). For larger lengths of the isolating, non-conjugated SAM part (aliphatic chains containing 4 and 6 hydrocarbon segments), the fill factor decreases due to higher series resistance. The hampered hole extraction led to current-voltage hysteresis in n=6 devices. For the methyl-substituted SAM, the optimum FF was reached with a chain length of n=4, while for nPACz, the highest FF was enabled by n=2. Possibly, self-assembly of the bare carbazole SAM nPACz is stabilized by pi-pi interactions of the carbazole fragments, whereas for the Me-substituted SAM an interplay between steric repulsion between the methyl fragments and van der Waals interaction between the hydrocarbon chains controls the SAM ordering and thus interface quality. This might cause the different optimum aliphatic chain lengths for the different SAM types. The new group of SAM molecules **Me-nPACz** demonstrated slightly better performance in PSC, compared with SAM systems developed by us earlier. With a maximum power conversion efficiency of ~21 % demonstrated by derivative with 4 carbon chain spacer **Me-4PACz**.

The PerTPV project has received funding from the European Union's Horizon 2020 research and innovation programme under grant agreement No 763977.

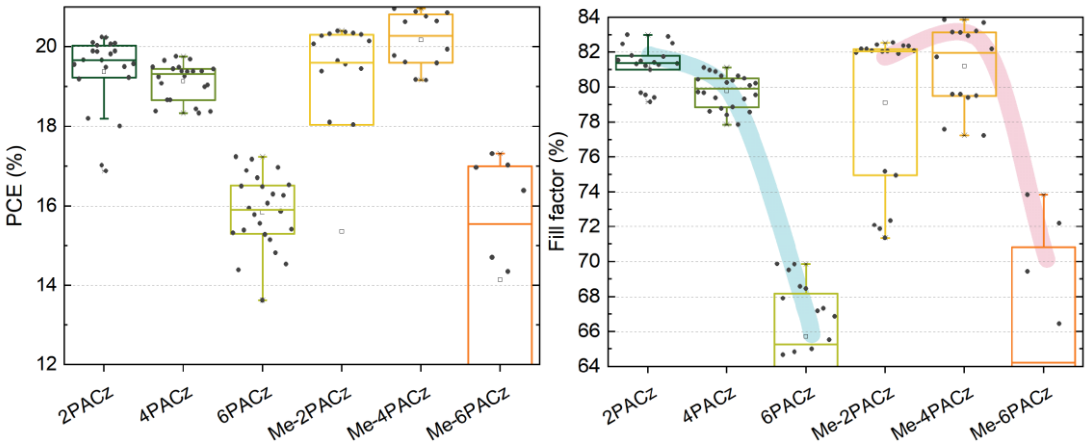

Figure 2.4. Influence of aliphatic chain length with bare and methyl-substituted carbazole SAMs on perovskite single-junction performance.

Suitability of the SAM approach for the construction of tandem devices was investigated using the monolithic perovskite/silicon tandem solar cell as initial testing platform. Tandem devices with carbazole SAMs outperformed widely used standard material PTAA (Figure 2.5), with best power conversion efficiency of 29.15% demonstrated by **Me-4PACz**.

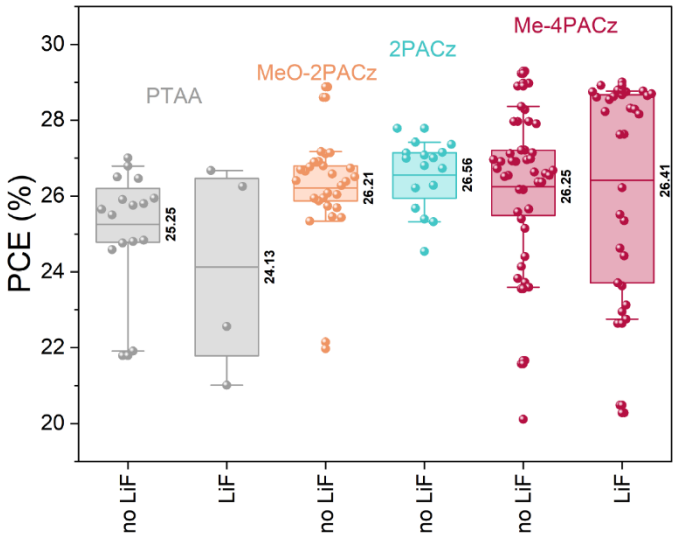

Figure 2.5. Performance of the carbazole SAMs in the monolithic perovskite/silicon tandem solar cells.

Devices with SAM hole selective layers also demonstrated very promising stability results. A non-encapsulated tandem cell with **Me-4PACz** retained 95.5% of its initial efficiency after 300 h of continuous maximum power point tracking in ambient air (Figure 2.6). Besides the long-term stability measurements at 25°C, an MPP track at elevated temperatures was conducted with a tandem cell containing dimethylcarbazole **Me-4PACz** (Figure 2.7). Following the procedure of Jost *et al.*, the temperature was successively increased from 25°C to 85°C and back to 25°C and there was no loss in PCE after this 200 minute procedure. We elucidate that the combination of efficient passivation at the hole selective interface and enhanced hole-extraction speed stabilize a perovskite absorber.

The PerTPV project has received funding from the European Union's Horizon 2020 research and innovation programme under grant agreement No 763977.

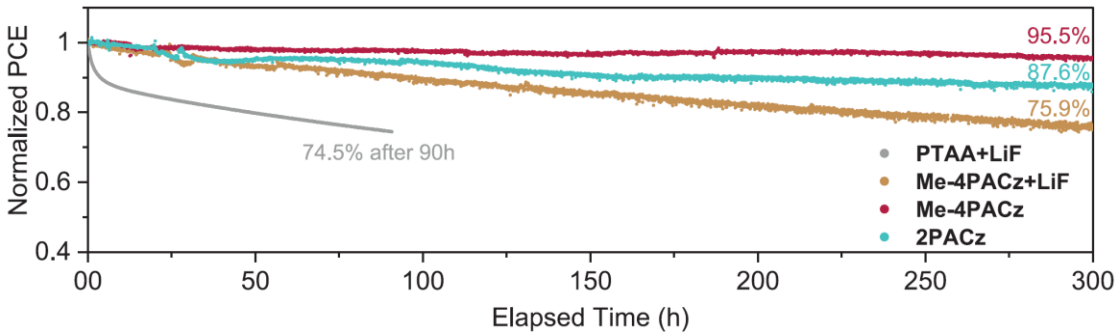

Figure 2.6. Long term MPP track using a dichromatic LED illumination of non-encapsulated solar cells in air at a controlled temperature of 25 °C. The data is normalized to the first 60 minutes of each individual track.

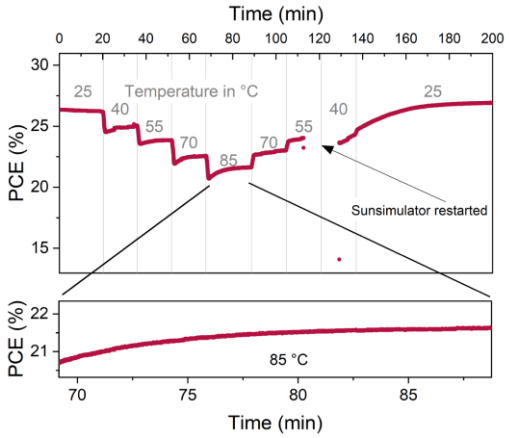

*Figure 2.7. MPP track of a tandem solar cell with **Me-4PACz**. The cell was illuminated with an AM1.5G spectrum. The cell was held for 15 minutes at 40 °C, 55 °C and 70 °C and for 20 minutes at 85 °C. Due to a technical issue, the sun simulator needed to be restarted. However, the cell was still exposed to the elevated temperature.*

3. Low band gap Pb:Sn Perovskite Cells

The chosen material for the narrow bandgap absorber is $FA_{0.83}Cs_{0.17}Pb_{0.5}Sn_{0.5}I_3$, which combines both narrow band gap and good thermal stability. Lead-tin materials that incorporate caesium (Cs) instead of methyl ammonium at the A -site have also shown superior stability under 1-sun max power point (MPP) tracking conditions[1]. We note that whilst more stable than compositions with higher percentages of tin, these materials still face issues with reproducibility. Most literature activity on high efficiency Pb:Sn perovskites relies of employing methylammonium as one of the cations. However, we have remained focussed on FA/Cs, due to the higher stability potential. Producing high performing Pb:Sn solar cells consistently, remains a challenge. Part of the work in this period has been to increase the breadth of activity on these materials and devices, by transferring the fabrication know-how to the project partners. This has helped us to trouble-shoot the sensitive areas and establish a more reproducible materials and device fabrication protocol.

The PerTPV project has received funding from the European Union's Horizon 2020 research and innovation programme under grant agreement No 763977.

3.1 Device fabrication and characteristics

Devices were fabricated using the p-i-n architecture consisting on ITO/PEDOT:PSS/(Pb-Sn perovskite)/$PC_{60}BM$/BCP/Ag, as detailed in Section 4.1. The devices were characterised as described in Section 4.2. This yields a champion device with a PCE of 18% and a steady-state power output of 17.5%, which we show in Figure 3.1.

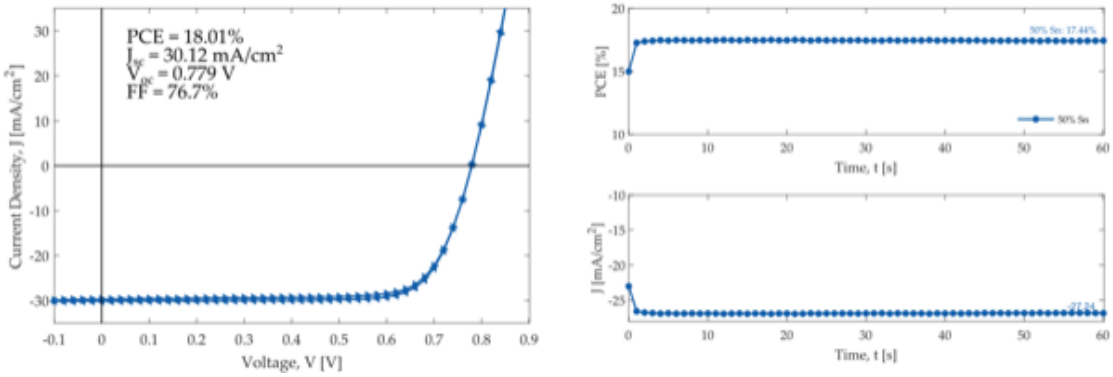

Figure 3.1. a) Current density vs. voltage (J-V) curves for the narrow bandgap lead-tin devices under 1-sun illumination at room temperature (RT) and the steady-state power conversion efficiency and maximum power point current density, measured over time.

3.2 Device processing know how transfer

The partners UVEG, CSEM and IIT all undertook activity to develop capability for fabrication of low band gap Pb:Sn perovskites. All activity was based on the same device structure and materials as described above, namely on ITO/PEDOT:PSS/($FA_{0.83}Cs_{0.17}Pb_{0.5}Sn_{0.5}I_3$)/$PC_{60}BM$/BCP/Ag. In Figure 3.2, we show the JV curves and performance of these cells. Partners are now able to fabricate Pb:Sn cells with power conversion efficiencies between 12 and 17%.

Low band gap perovskite solar cells processed at UVEG:
The solar cell structure processed at UVEG is *Glass / ITO / PEDOT:PSS 4083 (30 nm) / $FA_{0.7}MA_{0.3}Pb_{0.5}Sn_{0.5}I_3$ (about 700 nm) / C60 (20 nm) / BCP (7 nm) / Cu (100 nm)*

Perovskite precursor solution: FAI, MAI, PbI_2, SnI_2 (in 0.7:0.3:0.5:0.5 molar ratio) and 10 mol% of SnF_2 (relative to SnI_2) in DMF:DMSO 3:1 at 1.6 M, stirring for 2h at RT. 1x1 cm Sn foil added at the last 10 min. Perovskite deposition: Solvent engineering with 200 uL of precursor solution spin coated at 1000 rpm for 10s + 4000 rpm for 40s. 200 uL of anisole casted at sec 30. Annealed at 100 ºC for 10 min. Purge after every layer. The solar cells fabricated through this route operate reasonably efficiently, as shown in Figure 3.2, a power conversion efficiency of approximately 17% has been achieved.

The PerTPV project has received funding from the European Union's Horizon 2020 research and innovation programme under grant agreement No 763977.

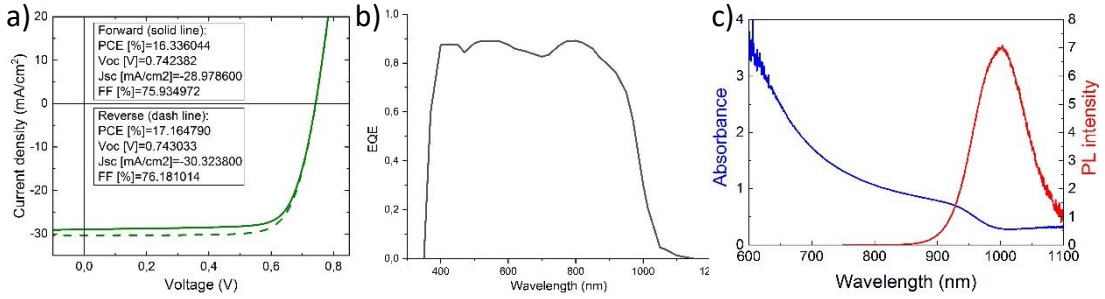

Figure 3.2. Performance of low bandgap Sn-Pb solar cells obtained by UVEG. Panel a) J-V curve under simulated AM1.5 sunlight in forward and reversed direction, inset shows key device parameters. Panel b), external quantum efficiency (EQE) as a function of wavelength. Panel c), absorbance (blue) and photoluminescence (red) spectra of the Sn-Pb perovskite.

Low bandgap perovskite solar cells processed at CSEM

Mixed Pb-Sn perovskite solar cells with composition $Cs_{0.25}FA_{0.75}Pb_{0.5}Sn_{0.5}I_3$ were fabricated at CSEM with structure ITO/PEDOT:PSS/Perovskite/C60/SnO2/Ag. A large improvement was found by addition of pieces of metallic tin to the perovskite solution shortly before processing. We show these results in Figure 3.3 below.

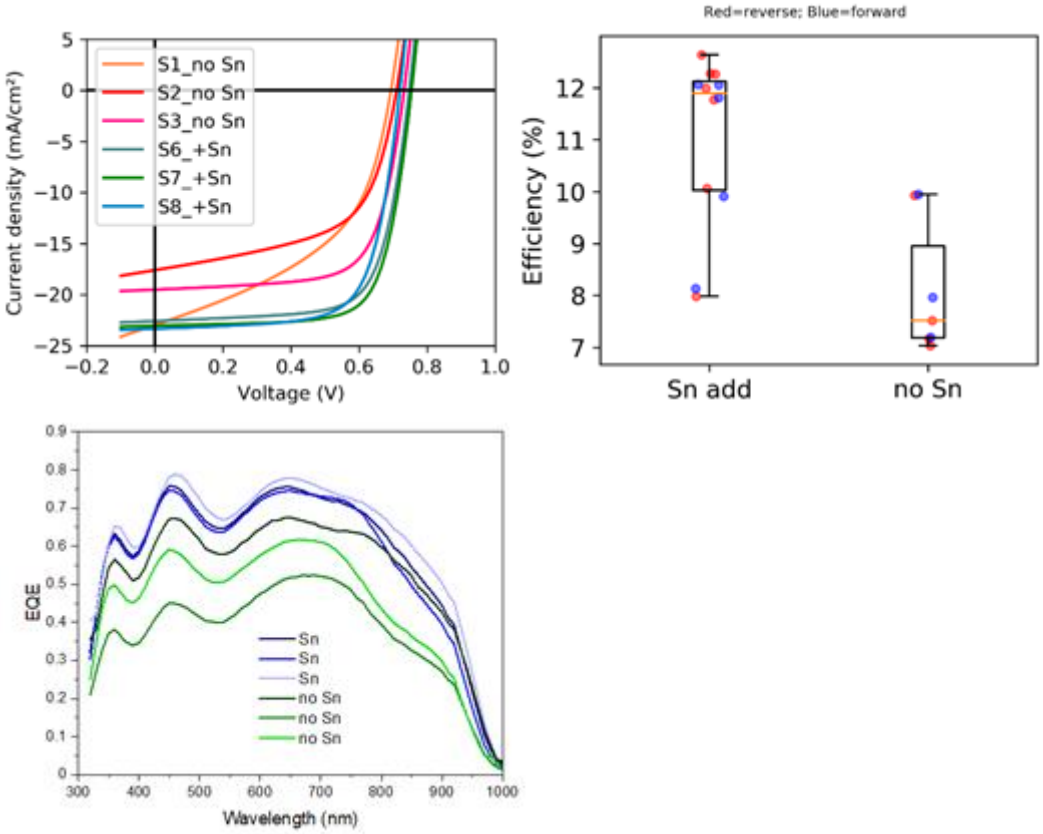

Figure 3.3 (a) JV curves at 1 sun of 1 cm^2 solar cells with and without addition of metallic tin to the perovskite solution. (b) Average efficiency of solar cells with and without addition of metallic tin. (c) EQE with and without addition of metallic tin.

The PerTPV project has received funding from the European Union's Horizon 2020 research and innovation programme under grant agreement No 763977.

The characteristic PV parameters for the best cells are reported in Table 3.1.

Composition	*E_g (eV)*	*J_{sc} (mA cm^{-2})*	*FF (%)*	*V_{oc} (mV)*	*PCE (%)*
$Cs_{0.25}FA_{0.75}PbI_3$ (w Sn)	1.25	23.04	72.66	755	12.63
$Cs_{0.25}FA_{0.75}PbI_3$ (w/o Sn)	1.25	23.18	70.91	719	11.81

4. Experimental Section

4.1 Device Fabrication

Solution processed solar cells:
For the low bandgap devices, we used a device stack of Glass/ITO/PEDOT:PSS/Perovskite/PCBM/BCP/Ag electrode. The ITO substrates (Shenzhen Huayu Union Technology Co Ltd, 10 ohm/sq) were cleaned via sonicating in a diluted Hellamanex solution (1% vol in DI water), deionized water, acetone, and isopropanol sequentially for 5 minutes each. The substrates were then treated with an O2 plasma process for 10 minutes. Poly(3,4-ethylenedioxythiophene) polystyrene sulfonate (Clevios P VP Al 4083, aqueous dispersion) solutions were prepared by diluting the as received PEDOT:PSS dispersion in MeOH in a 1:2 ratio respectively. Films were deposited on ITO via a static dispense of 180 µL followed by spinning at 4000 rpm for 40 seconds and subsequently annealed for 10 min at 150 ℃. These films were then transferred to a nitrogen film glovebox straightaway just before perovskite deposition. Perovskite films were fabricated by spin coating and the anti-solvent quenching method in a nitrogen filled glovebox. 100 µL of precursor solution was statically dispensed onto the substrate and the liquid meniscus was pulled over the substrate using the pipette tip to allow proper wetting before spinning the substrate at 3600 rpm for a total of 30 s. At 13 s 200 µL of anisole (the anti-solvent) was pipetted onto the middle of the spinning substrate with a dispense time of around 1 s. As soon as the chuck stopped a steady stream of nitrogen via a nitrogen gun was applied the surface of the film for a further 15 s. The films were then annealed at 100 ℃ for 10 min to give the resulting dark perovskite film. ([6,6]-Phenyl C61 butyric acid methyl ester, Solenne BV) solutions were prepared to a concentration of 20 mg/mL in a 3:1 mixture of chlorobenzene to dichlorobenzene. Once made, solutions were left for at least 24 h at room temperature before filtering with a 0.2 µm PTFE filter. PCBM was dynamically spin coated on top of the perovskite layer at 2000 rpm using 50 µL of solution and annealing for 1 minute at 100 ℃. (Bathocuproine, Sigma Aldrich) solutions prepared to a concentration of 0.5 mg/ml in isopropanol were stirred overnight at 70 °C and then filtered a 0.2 µm PTFE filter prior to use. BCP was dynamically spin coated on top of the perovskite layer at 5000 rpm using 70 µL of solution with no annealing. All electrodes for devices were deposited using a shadow mask to give an electrode pattern complimentary to our solar simulator. The pattern resulted in 8 pixels per substrate each with an active area of 0.0919 cm2. A Kurt J. Lesker Nano 36 evaporator was used to deposit 100nm silver electrodes by thermal evaporation under high vacuum (~10-6 mbar) at a rate of ~1.5nm/s.

For the wide bandgap devices we employed a device stack of Glass/FTO/polyTPD/perovskite/passivation/PCBM/BCP/Ag electrode. We use is 7

The PerTPV project has received funding from the European Union's Horizon 2020 research and innovation programme under grant agreement No 763977.

ohms/square fluorine-doped tin oxide (FTO) as a semi-transparent electrode. Substrates were cleaned in a similar manner to the low bandgap devices. The HTL is poly(N,N'-bis-4-butylphenyl-N,N'-bisphenyl) benzidine (polyTPD) doped with 2,3,5,6-Tetrafluoro-7,7,8,8-tetracyanoquinodimethane (F4TCNQ) in a ratio of 5:1 by weight. This was dissolved in toluene at a concentration of 1.2 mg/mL. 70 µL was dynamically deposited onto substrate at 2000rpm. After spinning for 20s, the films were annealed at 130 ℃ for 15 minutes. Perovskite films are fabricated by weighing formamidinium iodide (FAI), caesium iodide (CsI), lead iodide (PbI2) and lead bromide (PbBr2) stoichiometrically and dissolving in 4:1 by volume of N,N-dimethylformamide (DMF): Dimethyl sulfoxide (DMSO). 1-adamantane carboxylic acid (1AMCA) was dissolved in 4:1 by volume DMF:DMSO separately and added into the precursor solution. We vary the amount of 1AMCA in the precursor by changing the concentration of the additive solution, but adding a constant volume. In this way, we keep the concentration of the perovskite precursor constant, while varying the additive. The films were deposited by dynamically dropping 170 µL of precursor solution at 1000rpm. The speed increased to 5000rpm for 35s and 400 µL of anisole was dropped 5s before the end of the program. Films were then annealed at 100℃ for 40 minutes. We use Phenyl-C61-butyric acid methyl ester (PCBM) as the ETL at a concentration of 20mg/ml in 3:1 by volume chlorobenzene (CB):dichlorobenzene (DCB), prepared in the same way as in Section 4.1. PCBM was dynamically spin coated on top of the perovskite layer at 2000 rpm using 40 µL of solution and annealing for 3 minutes at 100 ℃. We use bathocuproine (BCP) as the HBL as previously described in Section 4.2.1. BCP was dynamically spin coated on top of the perovskite layer at 5000 rpm using 100 µL of solution with a 1 minute anneal at 100℃. Ag electrodes were finally deposited by thermal evaporation.

Vacuum deposited solar cells:
Materials. Photolithographically patterned ITO coated glass substrates were purchased from Naranjo Substrates (10 ohm/sq). Fullerene (C60) was purchased from Sigma Aldrich. TaTm was provided from Novaled GmbH. BCP, m-MTDATA, MoO3, MAI and FAI were purchased from Lumtec, CsI, PbI_2, and $PbBr_2$ from Tokyo Chemical Industry CO (TCI). All materials were used as received. ITO-coated glass substrates were subsequently cleaned with soap, water and isopropanol in an ultrasonic bath, followed by UV-ozone treatment. They were transferred to a vacuum chamber integrated into a nitrogen-filled glovebox and evacuated to a pressure of 10-6 mbar for the charge extraction front contact layer deposition. The vacuum chamber for organic deposition is equipped with two temperature-controlled evaporation sources (Creaphys) fitted with ceramic crucibles. Three quartz crystal microbalance (QCM) sensors are used, two monitoring the deposition rate of each evaporation source and a third close to the substrate holder monitoring the total deposition rate. A calibration factor was obtained by comparing the thickness inferred from the QCM sensors with that measured with a mechanical profilometer (Ambios XP1). Organics transport layers were co-sublimed at temperatures ranging from 160 ºC to 250 ºC, depending on the specific molecules. The vacuum chamber for perovskite deposition is equipped with four temperature-controlled evaporation sources (Creaphys) fitted with ceramic crucibles. Five quartz crystal microbalance (QCM) sensors are used, four monitoring the deposition rate of each evaporation source and a fifth close to the substrate holder monitoring the total deposition rate. During the perovskite deposition, the individual QCM reading for the 4 materials were kept stable and in a ratio depending on the desired final stoichiometry. Substrates were kept at room temperature during perovskite formation. Devices were finished with the deposition of the metal top contact (gold, 100 nm thick) in a third, dedicated vacuum chamber.

The PerTPV project has received funding from the European Union's Horizon 2020 research and innovation programme under grant agreement No 763977.

The device stack used for the wide bandgap solar cells is:
ITO/MoO3 (5 nm)/TaTm (10 nm)/ Cs0.25Fa0.75Pb(I0.78Br0.22)3 (500 nm)/C60 (25 nm)/BCP (7 nm)/Ag (100 nm)

4.2 Device Characterisation

Solution processed solar cells:
Current-voltage (JV) characteristics were recorded in ambient air under simulated AM1.5 solar light (1-Sun, 100 mW cm-2) generated by an ABET Class AAB sun 2000 simulator. Each device was measured with a 20 mV voltage step and a 100 ms time step (scan rate of 0.2 V/s). All devices were masked with a 0.0919 cm2 metal aperture to define the active area and eliminate edge effects. Stabilised power output (SPO) measurements were performed by holding the device at the voltage of the maximum power point, as determined by the JV characteristic, and monitoring the current density over the course of 60 s.

Vacuum deposited solar cells:
The external quantum efficiency (EQE) was estimated using the cell response at different wavelength (measured with a white light halogen lamp in combination with band-pass filters), where the solar spectrum mismatch is corrected using a calibrated Silicon reference cell (MiniSun simulator by ECN, the Netherlands). The current density-voltage (J-V) characteristics were obtained using a Keithley 2612A source measure under white light illumination using a solar simulator by Abet Technologies (model 10500 with an AM1.5G xenon lamp as the light source). The scan rate was 0.1 V/s. Before each measurement, the exact light intensity was determined using a calibrated Si reference diode equipped with an infrared cut-off filter (KG-3, Schott). The maximum power point tracking (MPPT) was evaluated inside a nitrogen filled glovebox illuminated under 1 sun illumination at 40 ºC with a Peltier temperature-control unit.

The PerTPV project has received funding from the European Union's Horizon 2020 research and innovation programme under grant agreement No 763977.